Cancer Immunology, Immunotherapy (2023) 72:1633–1646
https://doi.org/10.1007/s00262-022-03356-5

RESEARCH

Tumoral CD105 promotes immunosuppression, metastasis, and angiogenesis in renal cell carcinoma

Mariam Oladejo[1] · Hong-My Nguyen[1] · Hannah Seah[1] · Arani Datta[1] · Laurence M. Wood[1]

Received: 11 August 2022 / Accepted: 23 December 2022 / Published online: 31 December 2022

Abstract

CD105 (endoglin) is a transmembrane protein that functions as a TGF-beta coreceptor and is highly expressed on endothelial cells. Unsurprisingly, preclinical and clinical evidence strongly suggests that CD105 is an important contributor to tumor angiogenesis and tumor progression. Emerging evidence suggests that CD105 is also expressed by tumor cells themselves in certain cancers such as renal cell carcinoma (RCC). In human RCC tumor cells, CD105 expression is associated with stem cell-like properties and contributes to the malignant phenotype in vitro and in xenograft models. However, as a regulator of TGF-beta signaling, there is a striking lack of evidence for the role of tumor-expressed CD105 in the anti-tumor immune response and the tumor microenvironment. In this study, we report that tumor cell-expressed CD105 potentiates both the in vitro and in vivo tumorigenic potential of RCC in a syngeneic murine RCC tumor model. Importantly, we find that tumor cell-expressed CD105 sculpts the tumor microenvironment by enhancing the recruitment of immunosuppressive cell types and inhibiting the polyfunctionality of tumor-infiltrating $CD4^+$ and $CD8^+$ T cells. Finally, while CD105 expression by endothelial cells is a well-established contributor to tumor angiogenesis, we also find that tumor cell-expressed CD105 significantly contributes to tumor angiogenesis in RCC.

Keywords Renal cell carcinoma · CD105 · Endoglin · Tumor microenvironment · Angiogenesis

Introduction

Kidney cancer is the 8th most diagnosed type of cancer, accounting for approximately 4% of all new cancer cases in the USA [1]. Of all kidney cancer subtypes, renal cell carcinoma (RCC) is the most prominent. Further, RCC is the deadliest urological cancer, with 12% overall survival probability after metastasizing [2, 3]. Several factors contribute to the aggressive and metastatic nature of RCC, including vascularization, stemness, and resistance to therapy [4, 5].

CD105 (endoglin) is a 180 kDa transmembrane glycoprotein that serves as a co-receptor for the TGF-β signaling complex [6, 7]. CD105 is associated with angiogenesis in many cancer types since it is highly enriched in rapidly dividing endothelial cells [8–12]. In RCC, CD105 is expressed on both the tumor cells and the tumor-associated vasculature, and this expression correlates with reduced overall survival [13, 14].

A recent study suggests that tumoral expression of CD105 predicts a worse prognosis independent of its endothelial expression in RCC [13]. This prognostic value of tumor-associated CD105 is related, in part, to its role as a mediator of cancer stem cell-like properties [15–17]. However, the role of tumoral CD105 in regulating the diverse immune mechanisms that mediate tumor progression is still unclear. Solid tumors are highly heterogeneous, consisting of both malignant and diverse non-malignant cell types that can be pro- and anti-tumorigenic. In fact, TGF-β signaling regulates various physiological effects and is crucial for tumor progression and metastasis [18, 19].

The effect of tumoral CD105 on tumor progression in immunocompromised models has been well-characterized [16]. However, the role of tumor cell-expressed CD105 has not been fully explored in a relevant immunocompetent model. To address this, we generated a CD105-deficient murine RCC cell line and confirmed that CD105 regulates tumorigenicity in vitro and in vivo in syngeneic mice. Our results also demonstrate that the presence of CD105 impacts

✉ Laurence M. Wood
laurence.wood@ttuhsc.edu

[1] Department of Immunotherapeutics and Biotechnology, Jerry H Hodge School of Pharmacy, Texas Tech University Health Sciences Center, Abilene, TX, USA

the functionality of tumor-infiltrating T cells in the RCC tumor microenvironment (TME). Finally, our data support the hypothesis that tumoral CD105 recruits myeloid-derived suppressor cells (MDSCs) and tumor-associated macrophages (TAMs) into the TME to potentiate VEGF-induced angiogenesis.

Materials and methods

Cell line and culture

The murine RCC tumor cell line, Renca, was obtained from ATCC and cultured in RPMI media supplemented with 10% FBS and 1% penicillin/streptomycin at 37 °C and 5% CO_2. CD105 knockout cells were generated utilizing pCas-Guide-EF1a-GFP vector targeting the first exon of the murine CD105 gene. 48 hours post-transfection of the assembled p-Cas vector into semi-confluent Renca cells, GFP FACS sorting was carried out with a BD FACS sorter followed by single-cell cloning to select successfully edited cells.

Mice

Male Balb/c mice [6-8 weeks old] were purchased from The Jackson Laboratory (Bar Harbor, ME) and housed at the Texas Tech University Health Sciences Center (TTUHSC) Laboratory Animal Resource Center (LARC) in Abilene. All experiments were performed in accordance with the regulations of the TTUHSC Institutional Animal Care and Use Committee.

Quantitative polymerase chain reaction (qPCR)

RNA was extracted from respective tissues or cell lines with the Qiagen RNEasy Mini kit. Subsequently, 1ug of RNA was converted to cDNA using Applied Biosystem Reverse Transcription kit and quantitative PCR (qPCR) performed with Applied Biosystems Sybr Green Master mix and a Step One Plus Real-Time PCR system. Fold change was calculated using the ($2^{-\Delta\Delta ct}$) method, with all results normalized to 18s rRNA as the reference gene. Primers utilized in the study are shown in Supplementary Table 1.

Western blot

Cells were lysed with RIPA lysis buffer containing protease inhibitor cocktail. Lysates were cleared by centrifugation, mixed with NuPAGE LDS sample buffer, and reducing agent, boiled for 10 min, and separated by electrophoresis on a NuPAGE Bis–tris gel. Separated proteins were subsequently transferred to a PVDF membrane followed by blotting with primary antibody against murine CD105 (Biolegend clone: MJ7/18) and GAPDH (cell signaling, #5174) overnight at 4 °C. Blots were incubated with Streptavidin-HRP for CD105 and peroxidase-conjugated anti-rabbit antibody for GAPDH. Signal was developed with enhanced chemiluminescence (ThermoScientific) and visualized using a UVP imager.

Colony formation assay

10^3 wild-type control (Control) or CD105 knockout cells (crCD105) were plated in triplicate in a 6-well dish and cultured at 37 °C and 5% CO_2. Culture media were replenished every 72 h. After ten days, cells were fixed with methanol and stained with 0.01% gentian violet for 10 min. Images of each well were taken. Cell count and colony area were quantified using ImageJ.

Cell proliferation assay

2×10^4 of Control or crCD105 cells were plated in each well of a 96-well plate and cultured for 48 and 72 h. Cell proliferation was assessed using Cytoscan SRB Kit according to the manufacturer's protocol. The absorbance of each well was measured at 560 nm on a plate reader.

Transwell migration assay

4×10^4 of either Control or crCD105 Renca cells were seeded on the upper chamber of an 8um pore transwell insert. RPMI supplemented with 10% FBS was added to the lower chamber of the transwell system and cultured for 24 and 48 h at 37 °C and 5% CO_2. Subsequently, residual cells were removed from the upper chamber of the transwell insert, fixed with ethanol, and stained with 0.01% gentian violet. Migrated cells were imaged at three fields of view with the Cytation 5 imager, and the % area covered by migrated cells was quantified using ImageJ.

Scratch assay

5×10^5 of Control or crCD105 cells were allowed to reach confluency in a six-well plate and gap made with a p200 tip. The gap closure rate was monitored over 72 h, and images were taken at regular intervals using a confocal microscope. The gap area at each time point was analyzed using ImageJ and recorded as a % decrease from the baseline.

Tube formation assay

1×10^4 Control or crCD105 cells were plated in triplicate on a 96-well plate coated with 50ul Matrigel (Corning®) in the absence of serum for 6 h. Tube formation was observed

under a light microscope, images taken using the Cytation 5 imager, and tube branches were quantified using ImageJ.

Tumor challenge

1×10^6 of Control or crCD105 Renca cells were subcutaneously implanted into the flank of male Balb/c mice (n = 5/group). Tumor formation and progression were monitored every other day, and tumor volume was recorded and calculated as ($LxW^2 \div 2$)[20]. For the *orthotopic model,* 5×10^4 of either Control or crCD105 was implanted into the left kidney of mice as previously described [21]. After 20 days, kidneys and metastatic lungs were excised. Tumor weight was calculated by subtracting the weight of the healthy kidney from the diseased kidney. Kidney tumors were processed for downstream analysis, and lungs were fixed in Bouin's solution for 24 h, after which the fixative was replaced with 70% ethanol. Lung metastatic nodules were quantified and imaged with a Motin FEIN OPTIC SMZ-168 stereomicroscope connected to a ToupTek digital camera.

Flow cytometry

Excised tumors were processed into single-cell suspension by maceration through a 70-um cell strainer. 2×10^6 of the resultant cell suspension was either left unstimulated or stimulated with T cell Activation cocktail with Brefeldin A (Biolegend). Subsequently, cells were surface-stained with APC-Cy7-conjugated TCR-b, Percp-Cy5.5-conjugated CD4, Pe-Cy7-conjugated CD8, APC-conjugated-CD11b, PerCp-Cy5.5-conjugated-Gr-1, AF700-conjugated-CD11c, PE-conjugated-CD206, BV605-conjugated-CD45 or intracellularly stained with PE-conjugated-IFN-γ, AF700 conjugated-TNF-α, APC-conjugated-IL-2, and PE-conjugated-FoxP3. For the cell proliferation assay, 1×10^6 of either Control or crCD105 cells were stained with AF488 conjugated- Ki67 and PeCy7-conjugated-CD44. For the detection of CD105, 1×10^6 of either Control or crCD105 was stained with PeCy7-conjugated-CD105. Data were collected using BD LSR Fortessa flow cytometer, and results were analyzed using Flowjo 10.7 software. Antibodies were purchased from Biolegend and used at a dilution factor of 1:100 for intracellular stains and 1:200 for surface stains.

Immunohistochemistry and H&E

For immunohistochemistry, 10-um-thick paraffin-embedded lung sections were stained with anti-mouse CD8a (Cell signaling), and peroxidase-conjugated anti-rabbit antibody was used as the secondary reagent. Color was subsequently developed with DAB substrate (Vector laboratories). Slides were scanned with Aperio Scanscope, and positive staining in at least eight different fields was quantified by ImageJ. H&E staining was carried out as previously described [22].

Hemoglobin assay

1×10^6 or 1.2×10^6 of Control or crCD105 Renca cells, mixed with Matrigel (200ul of Matrigel and 100ul of cells), were injected s.c into the flank of male Balb/c mice. Tumors were monitored, and plugs were excised on Day 23. Excised plugs were processed in 10mls of RPMI media and centrifuged. The resultant pellet was lysed with 1 ml of ACK lysis buffer. Tumor RBC lysates were stored at -80^O prior to the hemoglobin assay. Hemoglobin content was measured with ThermoScientific Colorimetric Hemoglobin Detection Kit according to the manufacturer's protocol.

TCGA data analysis

The TCGA kidney cancer data were accessed and analyzed from the University of Alabama Cancer data analysis portal (http://ualcan.path.uab.edu./). Gene correlation analysis from the pan kidney cancer cohort was analyzed from the GEPIA 2 database (http://gepia2.cancer-pku.cn/).

Statistical analysis

All results are presented as parametric Student t tests except for survival plots which are shown as Mantel-Cox. Data were analyzed using GraphPad Prism software, and significant p values were depicted in the figures as follows, $*P < 0.05$, $**P < 0.01$, $***P < 0.001$, $****P < 0.0001$ ns $P > 0.05$. Error bars are shown as ± SEM.

Results

CD105 is highly expressed in RCC.

Based on the data obtained from The Cancer Genome Atlas and modified through UALCAN (http://ualcan.path.uab.edu./), CD105 expression is significantly elevated in primary RCC tumors in comparison with normal kidney tissue (Fig. 1A). In line with this, previous studies have demonstrated that elevated expression of CD105 in RCC correlates to a worse prognosis and predicts poorer outcomes [14, 23]. While the expression of CD105 has long been associated with vascular endothelial cells, recent studies have found expression of CD105 by human RCC tumor cell lines and tumor cells within clinical RCC tissues [13, 15, 16]. Since we seek to determine the role of tumor cell-expressed CD105 in a syngeneic mouse model of RCC, we assessed the expression of CD105 by the murine RCC tumor cell line, Renca. Much like in human RCC, CD105 is highly

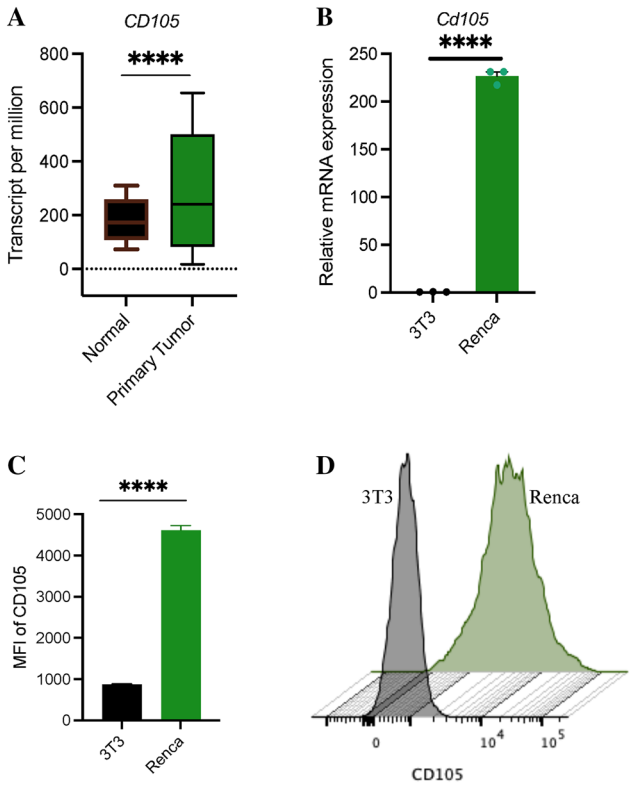

Fig. 1 CD105 is highly expressed in renal cell carcinoma. **A** Expression of CD105 between normal kidney tissues and primary tumor based on data obtained from TCGA. **B–D** Expression of CD105 between Renca and NIH-3T3. **B** mRNA expression of CD105. **C** Mean fluorescence intensity (MFI) of CD105. **D R**epresentative histograms of the expression of CD105

expressed by Renca in comparison with a non-transformed fibroblast cell line, 3T3 as determined by both qPCR and flow cytometry (Fig. 1B–D).

CD105 improves in vitro tumor proliferation but reduces in vitro tumor cell migration

To determine the role of tumoral CD105 expression on the malignant phenotype of RCC, we utilized CRISPR-Cas9 with CD105-targeting gRNAs to generate a CD105 knockout cell line, ***crCD105***, along with a control cell line utilizing the same plasmid with an irrelevant gRNA, *Control.* Knockout of CD105 in Renca was confirmed by Western blot and qPCR (Fig. 2A, B) To assess the impact of CD105 ablation on RCC tumor cell growth and proliferation, we carried out several assays to determine proliferative capacity. After plating out equivalent numbers of Control and crCD105 RCC tumor cells, a significant reduction in cell proliferation was found in crCD105 cells by an SRB assay after 48 and 72 h (Fig. 2C). A clonogenic assay confirmed our observation that deletion of CD105 reduces tumor cell proliferation as crCD105 cells display a significantly lower colony formation capacity compared to Control Renca cells as demonstrated by the number of colonies formed and the area covered by the colonies (Fig. 2D). We confirmed the above experiments with another CD105-deficient cell line (KD) that was generated by targeting a separate region of CD105 with CRISPR-Cas9 (Supplemental Fig. S1A–C). Since KD cells have a less robust CD105 deletion but displayed similar characteristics with crCD105, all subsequent experiments were carried out with crCD105.

Further, we performed intracellular staining of cells with a fluorophore-conjugated antibody against Ki67, a marker of cellular proliferation. The intensity of Ki67 was higher on the Control cells than on the crCD105 cells (Fig. 2E). While CD105 enhances the proliferative capacity of RCC tumor cells, this also enhances resistance to chemotherapeutic agents as previously reported in human RCC tumor cells [16]. We confirmed these observations in murine RCC as crCD105 Renca cells were more sensitive to cytotoxicity by doxorubicin and fludarabine than Control Renca tumor cells (Supplementary Fig. S2A-D). The role of CD105 in enhancing cell proliferation in RCC tumor cells could be due, in part, to its potentiation of a stem cell-like phenotype observed in human RCC tumor cells [16]. In fact, we find that CD105 depletion of Renca tumor cells results in a concomitant reduction in a marker of cancer cell stemness, CD44 (Fig. 2F) [16].

Migration is an essential step during cancer progression [24]. Since CD105 regulates cell migration and adhesion [25, 26], we sought to confirm whether this migratory character mediated by CD105 is maintained in the murine model of RCC. In a transwell migration assay, a significantly higher number of cells migrated toward a chemoattractant in the crCD105 Renca group than in the Control Renca group after 48 h (Fig. 2G). This enhanced migratory phenotype after CD105 depletion was confirmed in a scratch assay, where the crCD105 Renca cell line displayed a significantly higher gap closure rate than the Control Renca cell line (Fig. 2H).

CD105 enhances in vivo tumor growth and metastasis

Endothelial cell-associated CD105 and tumoral CD105 mediate different characteristics since endothelial CD105 promotes tumor progression by increasing vascularization and angiogenesis, and tumor cell-expressed CD105 is a cancer stem cell marker [15, 17, 27]. However, the effect of tumoral CD105 independent of its endothelial expression on in vivo tumor growth has not been evaluated in an immunocompetent model. To assess this, 1×10^6 cells of either Control or crCD105 cells were implanted subcutaneously in Balb/c mice. Interestingly, mice that were inoculated with crCD105 tumor cells initially demonstrated significantly enhanced tumorigenicity compared to those

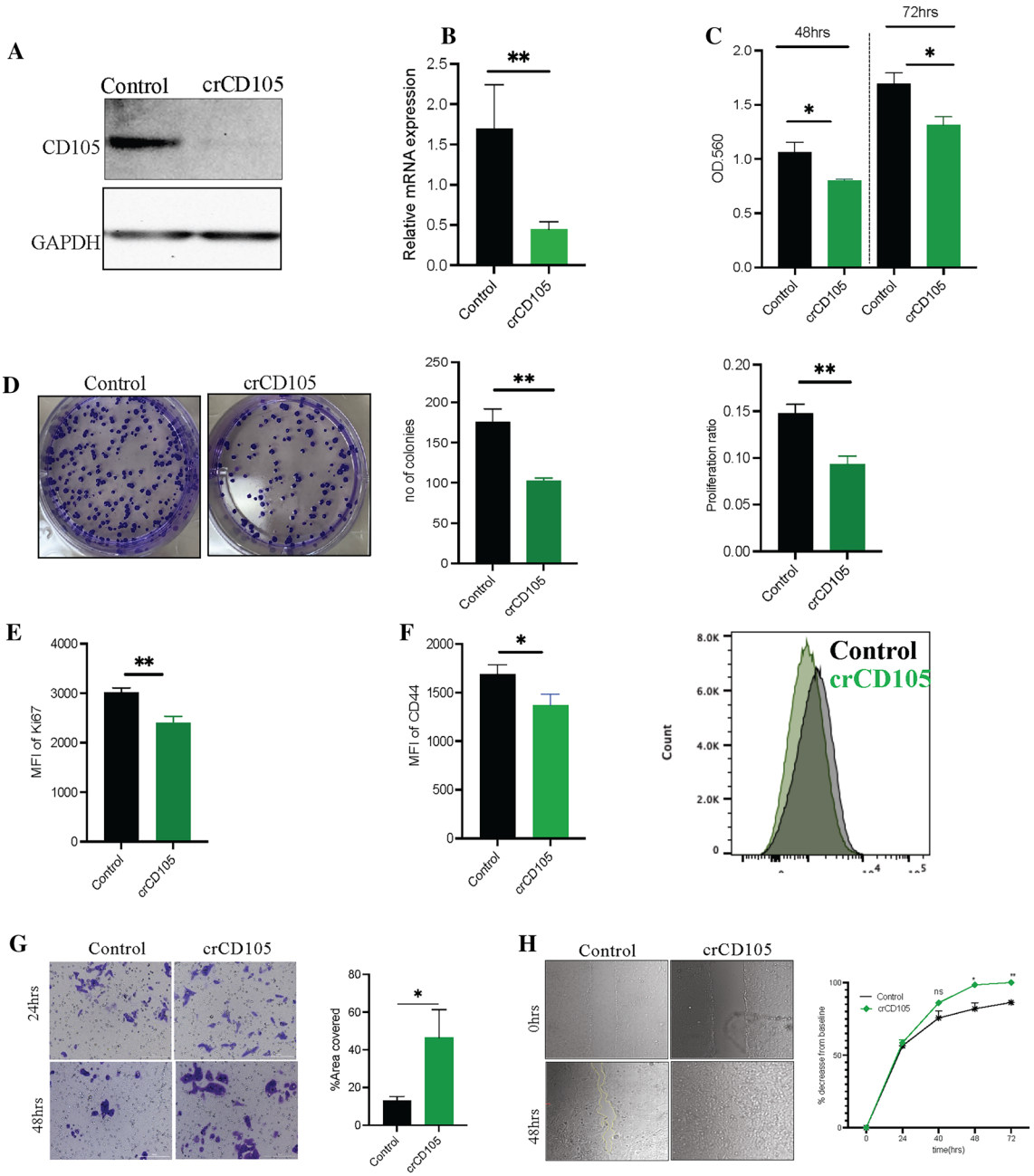

Fig. 2 Tumoral CD105 enhances tumor cell proliferation **A** protein and **B** mRNA expression of CD105 on Renca cells after treatment with a CD105-targeting CRISPR/Cas9 vector. **C** Comparison of growth rate between Control and crCD105 at 48 and 72 h. **D** Representative images of colony formation and statistical quantification of the number of colonies and proliferation ratio. The proliferation ratio is defined as the area covered by colonies/total area of well. **E** MFI of the proliferation marker ki67 and **F** MFI of CD44. **G** Representative image and statistical quantification of migrated cells in transwell migration assay. **H** Representative image and statistical quantification of scratch assay

that received Control cells (Fig. 3A). However, crCD105 tumor progression was stunted after nascent tumor formation, whereas Control tumor progression was significantly more rapid after formation (Fig. 3B–D). This result suggests that CD105 indeed supports tumor progression and higher tumor burden.

Since subcutaneous implantation may not sufficiently recapitulate the TME of RCC tumors developing within the kidney and does not provide information about

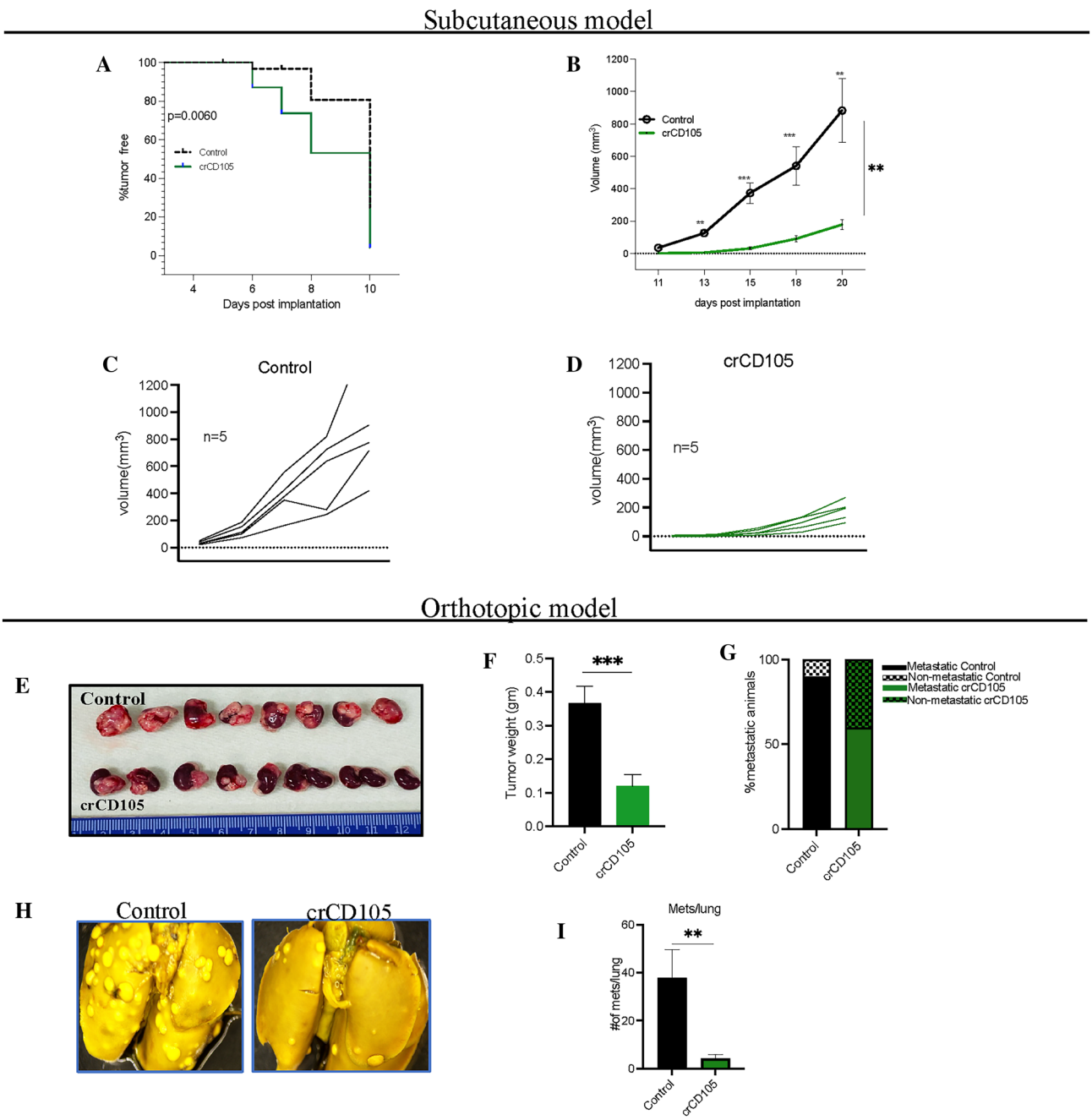

Fig. 3 Tumoral CD105 promotes in vivo tumor growth and metastasis **A** Kaplan–Meier plot for tumorigenicity. **B** Longitudinal tumor growth rate of subcutaneously implanted Control and crCD105 tumors. **C** The individual tumor growth pattern of Control and **D** CD105-deficient tumors. **E** Representative image of diseased kidneys from both the Control and crCD105 intra-renal tumor challenge groups. **F** Final tumor mass of orthotopic tumors. **G** Incidence of metastasis between Control and crCD105. **H** Representative image of metastatic nodules. **I** quantification of metastasis in the lungs

spontaneous metastasis, we utilized an orthotopic implantation model of RCC to confirm our findings [28, 29]. crCD105 or Control Renca cells were implanted into the left kidney of male Balb/c mice (n = 10/group) and monitored for 20 days. As in the subcutaneous model, there was a significant reduction in renal tumor formation and outgrowth in CD105-deficient tumor cells (Fig. 3E, F). Furthermore, we found that CD105 promoted metastasis as the incidence of lung metastasis was lower and the lung nodules were significantly reduced in the CD105-deficient

tumor cells in comparison with Control tumor-bearing mice (Fig. 3G–I, Supplementary Fig S4A).

Deletion of CD105 improves the functionality of tumor-infiltrating lymphocytes.

As CD105 is a co-receptor for the immunosuppressive cytokine TGF-beta, we sought to determine whether it's potentiation of tumor progression is linked to the suppression of functional anti-tumor immunity. To determine the role of tumoral CD105 in the anti-tumor T cell response, we investigated tumor-infiltrating T cell functionality in both crCD105 and Control s.c. tumor-bearing mice. Compared to Control tumors, crCD105 tumors demonstrated a significantly higher percentage of $CD8^+$ T cells producing anti-tumor inflammatory cytokines, including IFN-γ and TNF-α, but no significant difference in IL-2 production (Fig. 4A–C). In addition, $CD4^+$ T cells in the TME of crCD105 tumor tissues showed a higher population of cells producing IFN-γ, TNF-α, and IL-2 (Fig. 4F–H). As increased anti-tumor potential of tumor-infiltrating T cells is associated with multi-cytokine production, we sought to determine the proportion of tumor-infiltrating $CD8^+$ and $CD4^+$ T cells that were triple or double-cytokine producers. The $CD8^+$ cells in the TME of the crCD105 tumors showed a significantly higher population of $IFN\gamma^+IL\text{-}2^+TNF\alpha^+$(Fig. 4D, E). Also, the $IFN\gamma^+$ $TNF\alpha^+$ $CD8^+$ T cells were significantly higher in the CD105-deficient tumors than in the Control tumors (Fig. 4D, E). Similarly, for the $CD4^+$ T cell population, there was a significantly higher population of $IFN\gamma^+IL\text{-}2^+TNF\alpha^+$ triple producers and $IFN\gamma^+$ $IL\text{-}2^+$ double producers (Fig. 4I, J).

To confirm that a similar improvement in the TME was observed in the orthotopic tumors, we carried out immunophenotyping analysis. As in the subcutaneous model, crCD105 kidney tumor tissues displayed improved IFN-γ (Fig. 5A, F), TNF-α (Fig. 5B and G), and modest effect on IL-2 production (Fig. 5C, H) by both $CD8^+$ and $CD4^+$T cells. The polyfunctionality of these immune cells is further demonstrated by significantly higher multi-cytokine production ($IFN\gamma^+IL\text{-}2^+TNF\alpha^+$) by $CD8^+$ T cells (Fig. 5D, E) and $CD4^+$ T cells (Fig. 5I, J) and provides a rationale for the reduced tumor outgrowth in the CD105-deficient tumor tissues. Overall, the critical observation here is that deletion of CD105 polarized the TME toward a more immunologically "hot" phenotype.

CD105 promotes an immunosuppressive TME highly infiltrated with MDSCs and M2-TAMs

MDSCs play an important role in RCC progression [30, 31]. As in human RCC, the TME of the Renca model used herein is also characterized by heavy infiltration of MDSCs and TAMs [31]. Therefore, we investigated whether the deletion of CD105 impacts the proportion and phenotype of these immune cell populations. We found a significantly reduced population of $CD11b^+Gr1^+$ MDSCs in the orthotopically implanted CD105-deficient tumor tissues (Fig. 5K–M). This finding was substantiated in subcutaneously implanted CD105-deficient tumors as well (Fig. 6A–C). Importantly, a higher proportion of MDSCs found in Control tumors are monocytic MDSCs ($CD11b^{hi}Gr\text{-}1^{lo}$), a highly immunosuppressive subset (Figs. 5M, 6C). Furthermore, we observed that the TME of Control tumors was enriched with a higher population of myeloid lineage cells ($CD11b^+Gr\text{-}1^-$) than crCD105 tumors (Figs. 5N, 6D). These $CD11b^+Gr1^-$ cells displayed a higher population of conventional DCs ($CD11b^+CD11c^+$) (Fig. 6E), but a lower population of the M2-macrophage marker ($CD11b^+$ $CD206^+$) (Fig. 6F) in the TME of the CD105-deficient tumor tissues. To confirm that CD105 potentiates immunosuppression within the TME, we analyzed the expression of genes that are markers of TAMs. While there was not a significant difference in expression of genes associated with M1-TAM, there was a significant decrease in the expression of genes associated with the M2-macrophage phenotype (*Socs-2, Arg-1, Mgl-1*) in crCD105 tumors (Fig. 6G). Similarly, we found a significantly reduced population of $CD4^+Foxp3^+$ in the crCD105 tumors (Figs. 5O, Fig. 6I, J). Not surprisingly, the expression of immunosuppressive markers and cytokines, including *Il10, Tgf b*1*, pdcd1 and Mmp9* (Fig. 6H, J), was higher in Control tumors. To corroborate our results, we explored the publicly available TCGA database. We confirmed that increased expression of *Cd105* positively correlates with the expression of suppressive markers, including *Cd206 and Socs-2,* but negatively correlates with the expression of genes associated with a cytotoxic phenotype, such as *C2ta (MHC2)* (Supplementary Fig. S5A). Taken together, our results suggest that deletion of CD105 improves the landscape of the TME, rendering it less conducive to infiltration of MDSCs, M2-TAMs and potentially Tregs.

Tumoral CD105 contributes to RCC vascularization

The contribution of endothelial cell-expressed CD105 to angiogenesis is well established. However, it has not been thoroughly investigated whether this is solely dependent on the expression of CD105 by the endothelial cells or whether tumoral-expressed CD105 contributes to this effect. A previous study suggested that $CD105^+$ tumor cells can differentiate into an endothelial cell subtype [15]. Vasculogenic mimicry, commonly assayed as the formation of tubular structures on Matrigel, depicts a mechanism where differentiation of tumor cells with stem cell-like properties directly contributes to tumor vascularization [32]. Therefore, we carried out an in vitro vasculogenic assay to examine

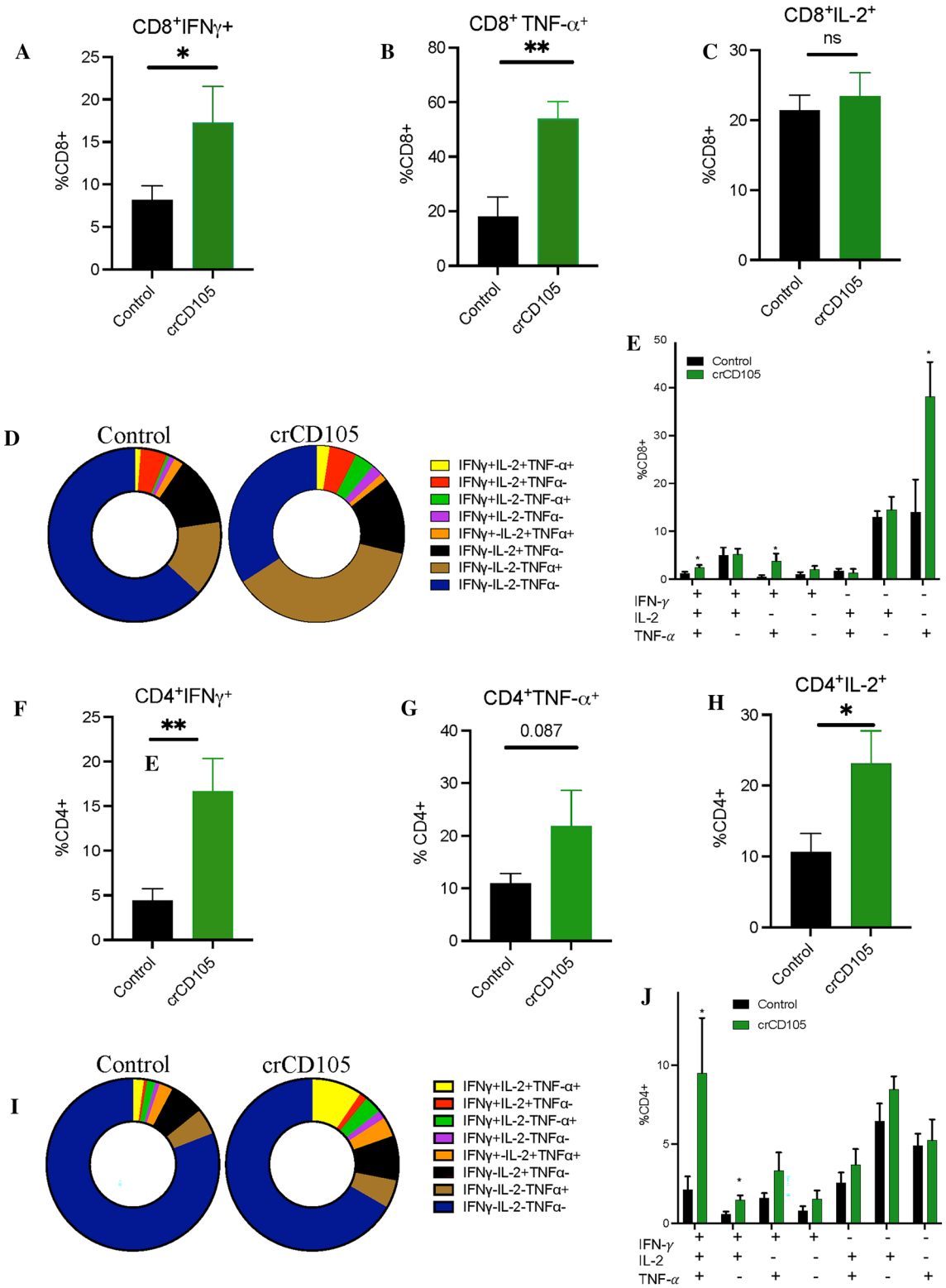

Fig. 4 Tumoral CD105 regulates the functionality of TIL in the subcutaneous TME Gating strategy for tumor-infiltrating lymphocytes, and cytokine production is as presented in Supplementary Figure S3A **A** IFN-γ, **B** TNF-α, **C** IL-2 producing CD8$^+$T cells. **D**, **E** Multicytokine production by CD8$^+$ T cells in the Control and crCD105 tumor tissues. **F**–**H** Population of **F** IFN-γ and **G** TNF-α and **H** IL-2 producing CD4$^+$ T cells. **I**, **J** Multicytokine production by CD4$^+$ T cells in the Control and crCD105 tumor tissues

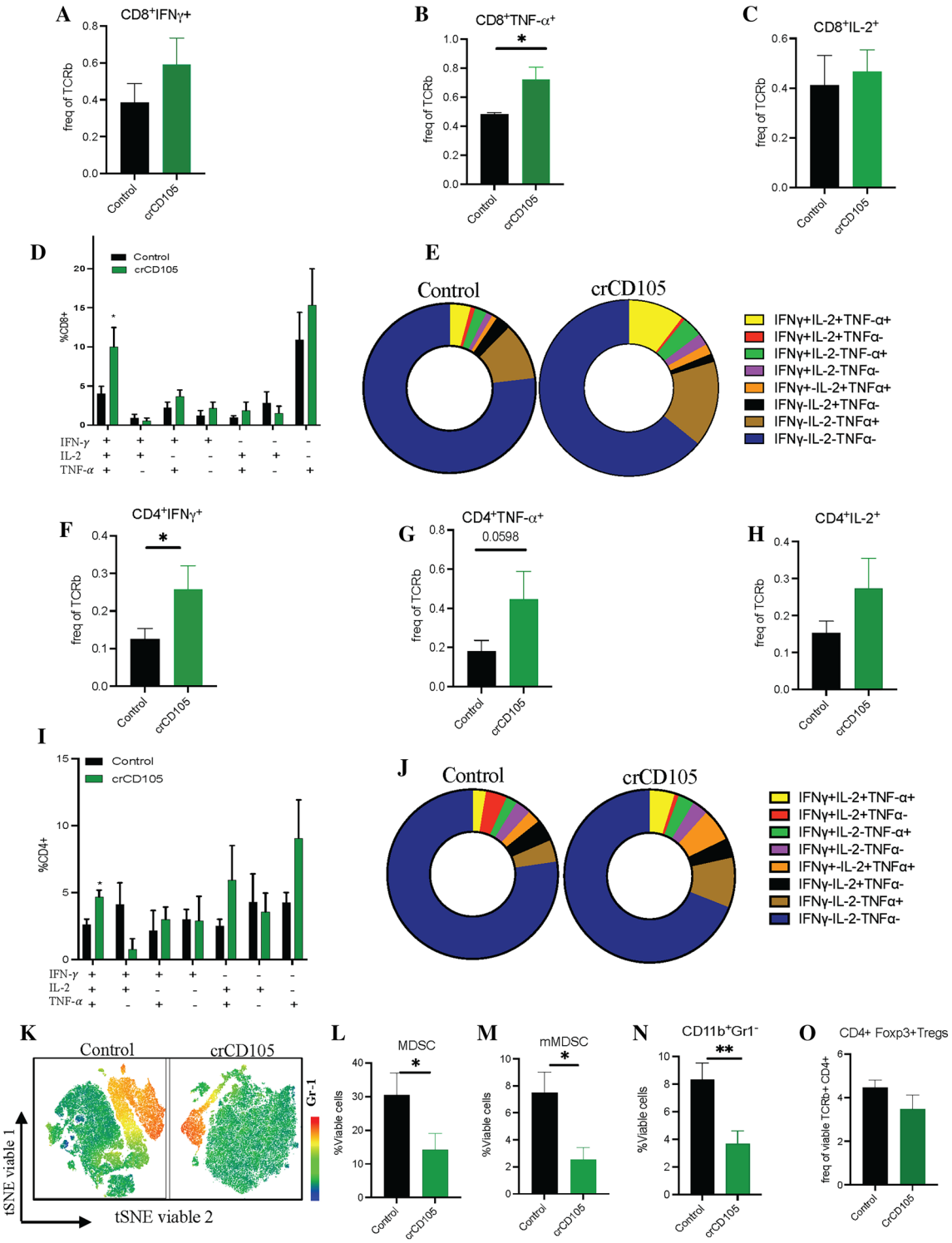

Fig. 5 Tumoral CD105 regulates the functionality of TIL in the orthotopic TME Gating strategy for tumor-infiltrating lymphocytes, and cytokine production is as presented in Supplementary Figure S3A. Production of **A** IFN-γ and **B** TNF-α and **C** IL-2 by the tumor-infiltrating $CD8^+$ T cells. **D**, **E** Multicytokine production by $CD8^+$ T cells in the Control and crCD105 tumor tissues. **F**–**H** The population of $CD4^+$ T cells producing **F** IFN-γ **G** TNF-α, and **H** IL-2. **I-J** Multicytokine production by $CD4^+$ T cells in the Control and crCD105 TME. **K** tSNE plots of Gr-1. Population of **L** $CD11b^+$ $Gr1^+$MDSCs **M** $CD11b+Gr1^{lo}$ cellsmMDSCs **N** myeloid population defined as $CD11b^+$ Gr-1^- and **O** $CD4^+$ $foxp3^+$ Tregs in the TME of Control in comparison with the crCD105 Renca tumors

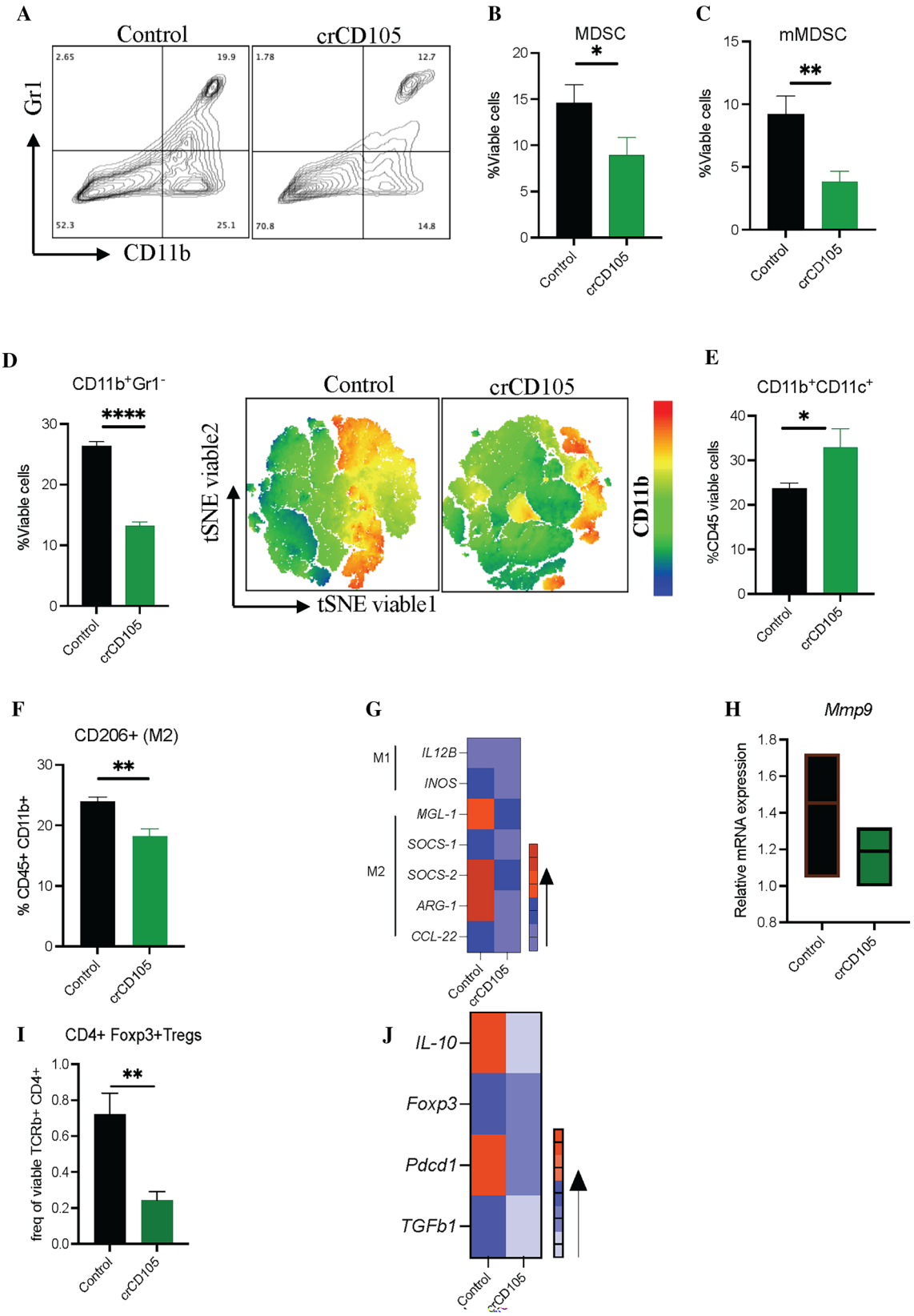
A
Control
crCD105
Gr1
CD11b
2.65
19.9
52.3
25.1
1.78
12.7
70.8
14.8
B
MDSC
*
%Viable cells
Control
crCD105
C
mMDSC
**
%Viable cells
Control
crCD105
D
CD11b+Gr1-
****
%Viable cells
Control
crCD105
Control
crCD105
tSNE viable2
tSNE viable1
CD11b
E
CD11b+CD11c+
*
%CD45 viable cells
Control
crCD105
F
CD206+ (M2)
**
% CD45+ CD11b+
Control
crCD105
G
M1
IL12B
INOS
M2
MGL-1
SOCS-1
SOCS-2
ARG-1
CCL-22
Control
crCD105
H
Mmp9
Relative mRNA expression
Control
crCD105
I
CD4+ Foxp3+Tregs
**
freq of viable TCRb+ CD4+
Control
crCD105
J
IL-10
Foxp3
Pdcd1
TGFb1
Control
crCD105

◂**Fig. 6** Tumor cell-expressed CD105 mediates suppression of the TME Gating strategy for MDSCs and TAMS is as presented in Supplementary Fig. 3A **and B A** Representative dot plots for MDSCs. The population of **B** $CD11b^{+}Gr1^{+}$ MDSCs and **C** $CD11b^{hi}Gr1^{lo}$ cells mMDSCs. **D** Quantification and tSNE plots of myeloid cells in the TME of Control tumor tissues as compared to the CD105-deficient tumor tissues. **E** Population of dendritic cells and **F** M2-like cells. **G** Heat map showing the expression of markers of M2-TAMs and **H** *Mmp9*, an MDSC recruiting cytokine in the TME **I** frequency of $CD4^{+}Foxp3^{+}$ cells to the TME **J** heat map of markers of immunosuppression including *Il-10,foxp3,pdcd1,* and *tgfb1* in the TME

the abilities of crCD105 or Control cells to form endothelial cell-like tubes [33]. After 6 h of plating respective cell lines on Matrigel, Control cells displayed extensive tube formation capacity, while crCD105 cells formed very few endothelial-like tubes (Fig. 7A, B). Since vasculogenesis and tube formation capacity are driven by *Vegfa*, [34] we examined the relative expression of *Vegfa* in both Control and crCD105 cell lines. In congruence with our vasculogenic assay results, we found a significantly higher expression of *Vegfa* in the Control cells in comparison with the crCD105 cells (Fig. 7C).

To translate our in vitro study into a clinically relevant model, we analyzed publicly available data from TCGA. We confirmed that the expression of CD105 by primary tumors positively correlates with the expression of angiogenic markers, including *Vegfa, Cd31*(Supplementary Fig S5B). Not surprisingly, the expression of CD105 does not correlate with *Vegfd*, a gene with a product primarily involved in lymphangiogenesis (Supplementary Fig S5B). We then evaluated the vascular density by quantifying the hemoglobin levels in the crCD105 or the Control tumor tissues, as shown in the schedule in Fig. 7D. Interestingly, we found significantly reduced hemoglobin levels in the crCD105 tumors compared to the Control tumors (Fig. 7E). Quantification of the expression of *Cd31* (Fig. 7F), *Vegfa* (Fig. 7G), and *Vegfd* (Fig. 7H) further confirmed the data observed from the TCGA data as we saw a significantly reduced expression of *Cd31* and *Vegfa* in the crCD105 tumors but no difference in the expression of *Vegfd.* Altogether, the data demonstrate that tumoral CD105 is involved in regulating vascularization and angiogenesis in conjunction with endothelial cell-expressed CD105.

Discussion

Endoglin is a complex protein involved in various cellular functions mediated by TGF-β signaling [35]. The effect of CD105 in RCC is even more complicated due to its expression by both tumor cells and endothelial cells [13]. While extensive reports have been made regarding the angiogenesis-inducing properties in endothelial cells [36], little is known about the function of tumor cell-expressed CD105. Recently, it has been suggested that tumor-expressed CD105 may serve as an independent prognostic factor in RCC [13]. Similarly, it has been postulated that tumor-expressed CD105 is involved in mediating stemness and chemoresistance of RCC tumors [15, 16]. Furthermore, these studies describe the possible implication of CD105 in epithelial–mesenchymal transition (EMT), including increased motility and invasiveness of CD105-expressing tumor cells. [17]. However, these studies did not investigate the implication of tumoral CD105 on the TME. The immune system plays a vital role in tumor growth characteristics and anti-tumor or pro-tumor responses; therefore, it is imperative to understand how tumoral CD105 perturbates the TME.

This current study investigated the role of tumor-expressed CD105 in tumorigenicity independent of its vasculature expression using a syngeneic mice model. Our observation that downregulation of CD105 supports tumor development but smaller and less vascularized tumors is consistent with what has been demonstrated in prostate carcinoma [37]. Further, our in vitro studies support previous findings that tumoral CD105 promotes a malignant phenotype characterized by clonogenicity, proliferation, stemness, and chemoresistance [16]. Interestingly, our study shows that CD105-expressing tumor cells migrate slower in a wound healing and transwell migration assay but showed increased metastasis in an orthotopic model of RCC. This result is consistent with what has been previously reported in prostate cancer and mouse fibroblasts over-expressing CD105 [26, 37, 38]**.** The reduction in in vivo metastasis in contrast to the in vitro metastatic potential could be the result of enhanced anti-tumor immunity as we observed improved $CD8^{+}$ T cell infiltration into the lungs of mice that were challenged with CD105-deficient Renca cells (Supplementary Fig. S4).

The TME of RCC is complex with infiltration of various immune cells, including TILs, MDSCs, cancer-associated fibroblasts (CAFs), and TAMs [39] Further, recent evidence has shown that attenuation of CD105 signaling by a monoclonal antibody, TRC105, reduces Treg infiltration into the TME [40]. Similarly, anti-endoglin monoclonal antibodies have been demonstrated to mediate their antitumor effect via $CD8^{+}$ T cells [41]. Further, Grange et al. demonstrated in vitro that CD105 + renal cancer cells and their derived exosomes interfered with optimal maturation of DCs and proliferation and activity of T cells [42]. Our results are in concert with these findings. We observed significant improvement in the functionality of $CD8^{+}$ and $CD4^{+}$ T cell subsets in the TME of CD105-deficient Renca tumors as characterized by enhanced multi-cytokine production in infiltrates of both subcutaneous and orthotopic tumors (Figs. 4 and 5A–H).

Furthermore, we found that tumor-expressed CD105 is important for the elevated infiltration of MDSCs and M2-TAMs in Renca tumors. The role of MDSC and TAMs

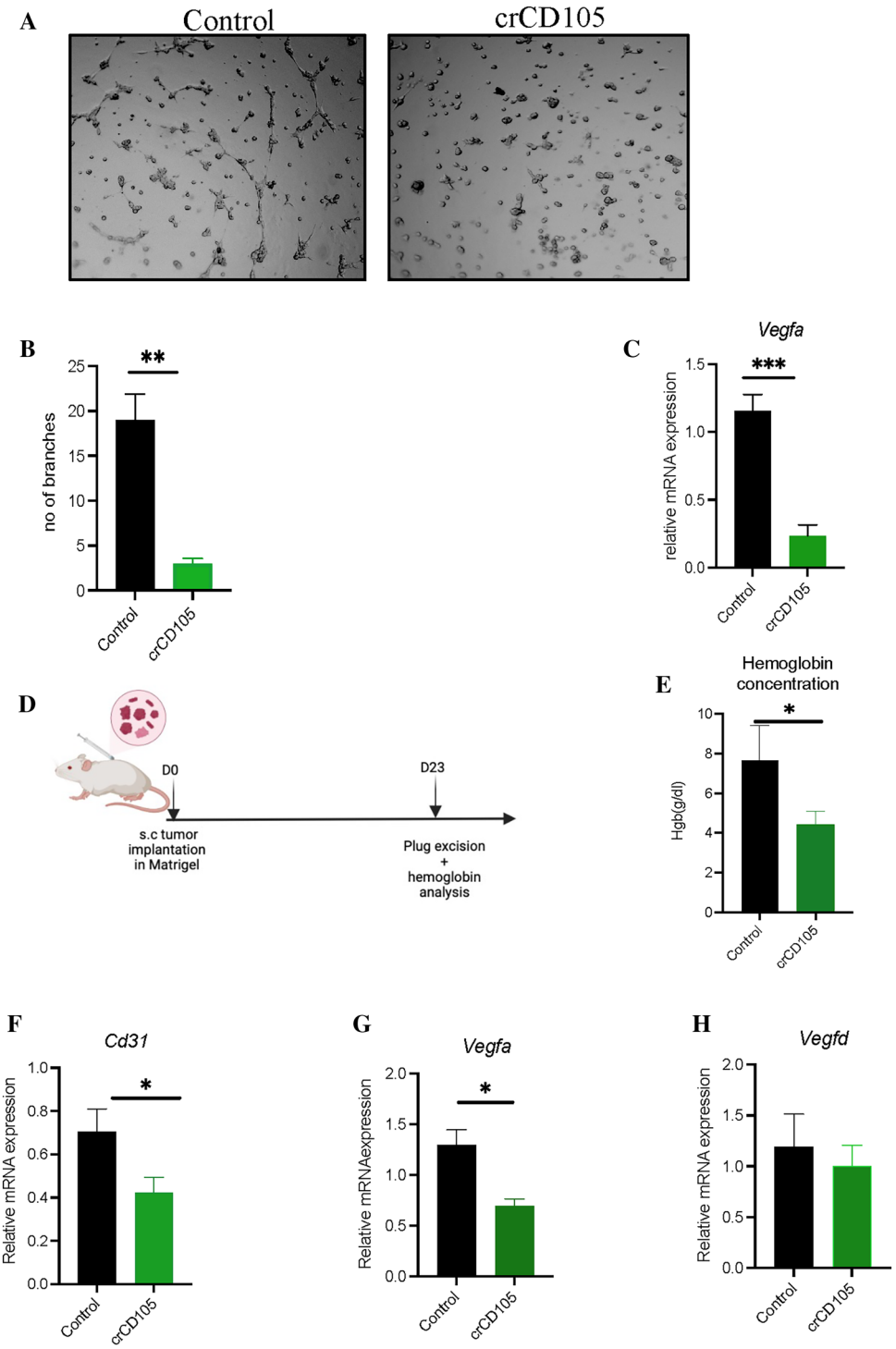

Fig. 7 Tumor cell-expressed CD105 contributes to intratumoral vasculogenesis and angiogenesis **A** Representative images for tube formation. **B** Quantification of the tube formation assay **C** mRNA expression of *Vegfa* by tumor cells. **D** Experimental schedule for Matrigel angiogenesis assay. **E** Quantification of hemoglobin content. mRNA expression of **F** *Cd31* and **G** *Vegfa* and **H** *Vegfd* between the tumor tissues from the CD105-deficient Renca cells and the Control Renca cells

in angiogenesis is well-documented [43, 44]. It has been demonstrated in various cancer models that Gr-1-expressing cells promote angiogenesis via VEGF and MMP-9 production [45], and this prompted us to investigate how tumoral CD105 affected tumor angiogenesis. We found that deletion of tumoral CD105 correlated with reduced vasculogenic and angiogenic potential both in vitro and in vivo, similar to what has been previously reported in the xenograft model (46). This suggests that tumoral CD105 modulates the expression of pro-angiogenic factors in the TME that likely synergize with endothelial CD105 expression to promote tumor angiogenesis in RCC.

To our knowledge, this is the first study to demonstrate the ability of tumoral CD105 to modulate tumorigenicity

and the TME in an immunocompetent model of RCC, with a potential synergistic effect on tumor vascularization. Therefore, strategies to manage RCC may benefit from understanding the diverse roles of tumor-expressed CD105 independent of its well-established endothelial cell-associated functions.

Supplementary Information The online version contains supplementary material available at https://doi.org/10.1007/s00262-022-03356-5.

Acknowledgements The authors thank Dr. Devin Lowe at the Department of Immunotherapeutics and Biotechnology, TTUHSC, for providing the CRISPR-Cas9 vector.

Author contributions LMW conceptualized the study. MO and LMW designed the experiments. MO carried out experiments, data analysis, preparation of figures, and manuscript drafting, HMN supported in orthotopic tumor modeling, HS performed scratch assay, and AD supported with FACS sorting. LMW acquired funding, provided supervision, and editing of the manuscript. All authors read and approved the final manuscript.

Funding This work is supported by the National Institutes of Health (NIH) 1R15CA216205-01 grant to Laurence Wood.

Data availability All data generated or analyzed during this study are included in the article and its supplementary information files.

Declarations

Conflict of interest The authors declare that they have no conflicting interests.

Ethical approval All applicable international, national, and institutional standards for the care and use of experimental animals were followed. All studies involving animals were carried out in accordance with ethical standards of the Texas Tech University Health Sciences Center under the IACUC protocol number 17018.

References

1. Kidney and Renal Pelvis Cancer [Internet]. Available from: https://seer.cancer.gov/statfacts/html/kidrp.html.
2. Padala SA, Barsouk A, Thandra KC, Saginala K, Mohammed A, Vakiti A et al (2020) Epidemiology of renal cell carcinoma. World J Oncol 11(3):79–87
3. Capitanio U, Bensalah K, Bex A, Boorjian SA, Bray F, Coleman J et al (2019) Epidemiology of renal cell carcinoma. Eur Urol 75(1):74–84
4. Stubbs C, Bardoli AD, Afshar M, Pirrie S, Miscoria M, Wheeley I et al (2017) A study of angiogenesis markers in patients with renal cell carcinoma undergoing therapy with sunitinib. Anticancer Res 37(1):253–259
5. Mertz KD, Demichelis F, Kim R, Schraml P, Storz M, Diener PA et al (2007) Automated immunofluorescence analysis defines microvessel area as a prognostic parameter in clear cell renal cell cancer. Hum Pathol 38(10):1454–1462
6. Barbara NP, Wrana JL, Letarte M (1999) Endoglin is an accessory protein that interacts with the signaling receptor complex of multiple members of the transforming growth factor-beta superfamily. J Biol Chem 274(2):584–594
7. Cheifetz S, Bellon T, Cales C, Vera S, Bernabeu C, Massague J et al (1992) Endoglin is a component of the transforming growth factor-beta receptor system in human endothelial cells. J Biol Chem 267(27):19027–19030
8. Nogues A, Gallardo-Vara E, Zafra MP, Mate P, Marijuan JL, Alonso A et al (2020) Endoglin (CD105) and VEGF as potential angiogenic and dissemination markers for colorectal cancer. World J Surg Oncol 18(1):99
9. Dales JP, Garcia S, Bonnier P, Duffaud F, Andrac-Meyer L, Ramuz O et al (2003) CD105 expression is a marker of high metastatic risk and poor outcome in breast carcinomas. Correlations between immunohistochemical analysis and long-term follow-up in a series of 929 patients. Am J Clin Pathol 119(3):374–80
10. Jeng KS, Sheen IS, Lin SS, Leu CM, Chang CF (2021) The role of endoglin in hepatocellular carcinoma. Int J Mol Sci 22(6):3208
11. Xu Y, Wang D, Zhao LM, Zhao XL, Shen JJ, Xie Y et al (2013) Endoglin is necessary for angiogenesis in human ovarian carcinoma-derived primary endothelial cells. Cancer Biol Ther 14(10):937–948
12. Momoi Y, Nishida J, Miyakuni K, Kuroda M, Kubota SI, Miyazono K et al (2021) Heterogenous expression of endoglin marks advanced renal cancer with distinct tumor microenvironment fitness. Cancer Sci 112(8):3136–3149
13. Saroufim A, Messai Y, Hasmim M, Rioux N, Iacovelli R, Verhoest G et al (2014) Tumoral CD105 is a novel independent prognostic marker for prognosis in clear-cell renal cell carcinoma. Br J Cancer 110(7):1778–1784
14. Saeednejad Zanjani L, Madjd Z, Abolhasani M, Shariftabrizi A, Rasti A, Asgari M (2018) Expression of CD105 cancer stem cell marker in three subtypes of renal cell carcinoma. Cancer Biomark 21(4):821–837
15. Bussolati B, Bruno S, Grange C, Ferrando U, Camussi G (2008) Identification of a tumor-initiating stem cell population in human renal carcinomas. FASEB J 22(10):3696–3705
16. Hu J, Guan W, Liu P, Dai J, Tang K, Xiao H et al (2017) Endoglin is essential for the maintenance of self-renewal and chemoresistance in renal cancer stem cells. Stem Cell Reports 9(2):464–477
17. Hu J, Guan W, Yan L, Ye Z, Wu L, Xu H (2019) Cancer stem cell marker endoglin (CD105) induces epithelial mesenchymal transition (EMT) but not metastasis in clear cell renal cell carcinoma. Stem Cells Int 2019:9060152
18. Rich JN (2016) Cancer stem cells: understanding tumor hierarchy and heterogeneity. Medicine 95(1 Suppl 1):S2–S7
19. Pasche B (2001) Role of transforming growth factor beta in cancer. J Cell Physiol 186(2):153–168
20. Faustino-Rocha A, Oliveira PA, Pinho-Oliveira J, Teixeira-Guedes C, Soares-Maia R, da Costa RG et al (2013) Estimation of rat mammary tumor volume using caliper and ultrasonography measurements. Lab Anim 42(6):217–224
21. Murphy KA, James BR, Wilber A, Griffith TS (2017) A syngeneic mouse model of metastatic renal cell carcinoma for quantitative and longitudinal assessment of preclinical therapies. J Vis Exp 122:e55080
22. Feldman AT, Wolfe D (2014) Tissue processing and hematoxylin and eosin staining. Methods Mol Biol 1180:31–43
23. Dubinski W, Gabril M, Iakovlev VV, Scorilas A, Youssef YM, Faragalla H et al (2012) Assessment of the prognostic significance of endoglin (CD105) in clear cell renal cell carcinoma using automated image analysis. Hum Pathol 43(7):1037–1043
24. Bravo-Cordero JJ, Hodgson L, Condeelis J (2012) Directed cell invasion and migration during metastasis. Curr Opin Cell Biol 24(2):277–283
25. Guo B, Rooney P, Slevin M, Li C, Parameshwar S, Liu D et al (2004) Overexpression of CD105 in rat myoblasts: role of CD105 in cell attachment, spreading and survival. Int J Oncol 25(2):285–291

26. Guerrero-Esteo M, Lastres P, Letamendia A, Perez-Alvarez MJ, Langa C, Lopez LA et al (1999) Endoglin overexpression modulates cellular morphology, migration, and adhesion of mouse fibroblasts. Eur J Cell Biol 78(9):614–623
27. Duff SE, Li C, Garland JM, Kumar S (2003) CD105 is important for angiogenesis: evidence and potential applications. FASEB J 17(9):984–992
28. Devaud C, Westwood JA, John LB, Flynn JK, Paquet-Fifield S, Duong CP et al (2014) Tissues in different anatomical sites can sculpt and vary the tumor microenvironment to affect responses to therapy. Mol Ther 22(1):18–27
29. Sobczuk P, Brodziak A, Khan MI, Chhabra S, Fiedorowicz M, Welniak-Kaminska M et al (2020) Choosing the right animal model for renal cancer research. Transl Oncol 13(3):100745
30. Rodriguez PC, Ernstoff MS, Hernandez C, Atkins M, Zabaleta J, Sierra R et al (2009) Arginase I-producing myeloid-derived suppressor cells in renal cell carcinoma are a subpopulation of activated granulocytes. Cancer Res 69(4):1553–1560
31. Finke JH, Rayman PA, Ko JS, Bradley JM, Gendler SJ, Cohen PA (2013) Modification of the tumor microenvironment as a novel target of renal cell carcinoma therapeutics. Cancer J 19(4):353–364
32. Serova M, Tijeras-Raballand A, Dos Santos C, Martinet M, Neuzillet C, Lopez A et al (2016) Everolimus affects vasculogenic mimicry in renal carcinoma resistant to sunitinib. Oncotarget 7(25):38467–38486
33. You B, Sun Y, Luo J, Wang K, Liu Q, Fang R et al (2021) Androgen receptor promotes renal cell carcinoma (RCC) vasculogenic mimicry (VM) via altering TWIST1 nonsense-mediated decay through lncRNA-TANAR. Oncogene 40(9):1674–1689
34. Xie C, Schwarz EM, Sampson ER, Dhillon RS, Li D, O'Keefe RJ et al (2012) Unique angiogenic and vasculogenic properties of renal cell carcinoma in a xenograft model of bone metastasis are associated with high levels of vegf-a and decreased ang-1 expression. J Orthop Res 30(2):325–333
35. Goumans MJ, Liu Z, ten Dijke P (2009) TGF-beta signaling in vascular biology and dysfunction. Cell Res 19(1):116–127
36. Nassiri F, Cusimano MD, Scheithauer BW, Rotondo F, Fazio A, Yousef GM et al (2011) Endoglin (CD105): a review of its role in angiogenesis and tumor diagnosis, progression and therapy. Anticancer Res 31(6):2283–2290
37. Romero D, O'Neill C, Terzic A, Contois L, Young K, Conley BA et al (2011) Endoglin regulates cancer-stromal cell interactions in prostate tumors. Cancer Res 71(10):3482–3493
38. Liu Y, Jovanovic B, Pins M, Lee C, Bergan RC (2002) Over expression of endoglin in human prostate cancer suppresses cell detachment, migration and invasion. Oncogene 21(54):8272–8281
39. Zhang S, Zhang E, Long J, Hu Z, Peng J, Liu L et al (2019) Immune infiltration in renal cell carcinoma. Cancer Sci 110(5):1564–1572
40. Schoonderwoerd MJA, Koops MFM, Angela RA, Koolmoes B, Toitou M, Paauwe M et al (2020) Targeting endoglin-expressing regulatory T cells in the tumor microenvironment enhances the effect of PD1 checkpoint inhibitor immunotherapy. Clin Cancer Res 26(14):3831–3842
41. Tsujie M, Tsujie T, Toi H, Uneda S, Shiozaki K, Tsai H et al (2008) Anti-tumor activity of an anti-endoglin monoclonal antibody is enhanced in immunocompetent mice. Int J Cancer 122(10):2266–2273
42. Grange C, Tapparo M, Tritta S, Deregibus MC, Battaglia A, Gontero P et al (2015) Role of HLA-G and extracellular vesicles in renal cancer stem cell-induced inhibition of dendritic cell differentiation. BMC Cancer 15:1009
43. Yin JH, Liu CS, Yu AP, Yao JQ, Shen YJ, Cao JP (2018) Pro-angiogenic activity of monocytic-type myeloid-derived suppressor cells from Balb/C mice infected with echinococcus granulosus and the regulatory role of miRNAs. Cell Physiol Biochem 51(3):1207–1220
44. Riabov V, Gudima A, Wang N, Mickley A, Orekhov A, Kzhyshkowska J (2014) Role of tumor associated macrophages in tumor angiogenesis and lymphangiogenesis. Front Physiol 5:75
45. Bergers G, Brekken R, McMahon G, Vu TH, Itoh T, Tamaki K et al (2000) Matrix metalloproteinase-9 triggers the angiogenic switch during carcinogenesis. Nat Cell Biol 2(10):737–744
46. Fiedorowicz M, Khan MI, Strzemecki D, Orzel J, Welniak-Kaminska M, Sobiborowicz A et al (2020) Renal carcinoma CD105-/CD44- cells display stem-like properties in vitro and form aggressive tumors in vivo. Sci Rep 10(1):5379